Sensors and Actuators B 248 (2017) 753–760

Contents lists available at ScienceDirect

Sensors and Actuators B: Chemical

journal homepage: www.elsevier.com/locate/snb

Research Paper

Top-and-side dual-view microfluidic device with embedded prism

Yuto Kazama[a], Edwin T. Carlen[b,c], Albert van den Berg[c], Akihide Hibara[d,e,*]

[a] Institute of Industrial Science, The University of Tokyo, Japan
[b] Graduate School of Pure and Applied Sciences, University of Tsukuba, Japan
[c] MESA+, University of Twente, The Netherlands
[d] Institute of Multidisciplinary Research for Advanced Materials, Tohoku University, Japan
[e] Department of Chemistry, Graduate School of Science, Tokyo Institute of Technology, Japan

ARTICLE INFO

Article history:
Received 24 January 2017
Received in revised form 3 March 2017
Accepted 4 April 2017
Available online 12 April 2017

Keywords:
Dual view
Microfluidic channel
PDMS
Dark-field view
Fluorescence

ABSTRACT

A polydimethylsiloxane microfluidic device enabling dual-view visualization is proposed and demonstrated. A prism with a 2 mm square base was embedded beside a 300 μm-wide microchannel. In addition to ordinary visualization from the top of the device, the microchannel could be viewed from the side, and its optical path was reflected to the top by the prism. The top and side dual visualization in a single field of view was then realized with a single objective lens. The shifts in the focal point in the top and side directions were modeled, and a compensation method utilizing a flat sheet was used. After simultaneous bright-field and dark-field visualization was attained, dual-view fluorescence imaging of the fluorescent solution and cells was realized.

1. Introduction

Microfluidic and nanofluidic systems have been enthusiastically investigated in last two decades [1–9]. The optical microscope is an important tool for studying micro- and nanofluidic devices [10–14]; it has various observation modes, such as a bright-field, dark-field, and fluorescence modes, and appropriate modes are chosen depending on the situation. For example, the dark-field mode is effective for immobilized particles.

In microfluidic investigations and applications, parameters such as three-dimensional (3D) position, shape, and deformation are often examined. One of the most common 3D imaging methods is the confocal fluorescent microscope, which can visualize microscale objects and flows with high resolution. For deformable samples such as microdroplets, the holographic 3D imaging method has been used [15,16]. For example, Oishi et al. demonstrated 3D visualization of the droplet-formation process by utilizing their digital holographic microscope. These methods utilize a coherent light source and 3D visualization is achieved with ordinary optical setups, namely a combination of an illumination path and an observation path.

Another possible 3D visualization approach is the stereoscope, with which microscale objects are observed from two different directions, without requiring a coherent light source. An ordinary binocular stereomicroscope with a slight angle difference may appear simple to our eyes, but 3D visual recording is not easy and image reconstruction methods, such as the digital image correlation method [17], are still under development. One simple way to facilitate dual-direction observation is to observe from the orthogonal directions to obtain a combined image like an orthographic projection. If orthographic-projection-like imaging is easily available, it may become a feasible option for 3D visualization.

Polydimethylsiloxane (PDMS) is widely used in microfluidic technologies and occasionally used for optofluidic devices [18,19] and for embedding small objects in microfluidic devices [20–24]. Recently, we have investigated an optics-embedding technique in PDMS microfluidic devices [25–27]. This method can potentially be applied to 3D visualization, as shown in Fig. 1. In this design, a prism is embedded beside a microchannel and an image from the side plane of the microchannel is obtained by utilizing reflection in the prism. The side-view image was obtained in our previous work [25,26], but, because of the difference between the focal lengths for the top and side observations, simultaneous top-and-side (dual) view image has not been realized.

Here we propose and demonstrate a new microfluidic device that offers simultaneous top-and-side (dual) views. The difference between the focal lengths of the top- and side-view paths is com-

* Corresponding author at: IMRAM, Tohoku University, 2-1-1 Katahira, Aoba, Sendai, 980-8577, Japan.
E-mail address: hibara@tagen.tohoku.ac.jp (A. Hibara).

http://dx.doi.org/10.1016/j.snb.2017.04.013
0925-4005/

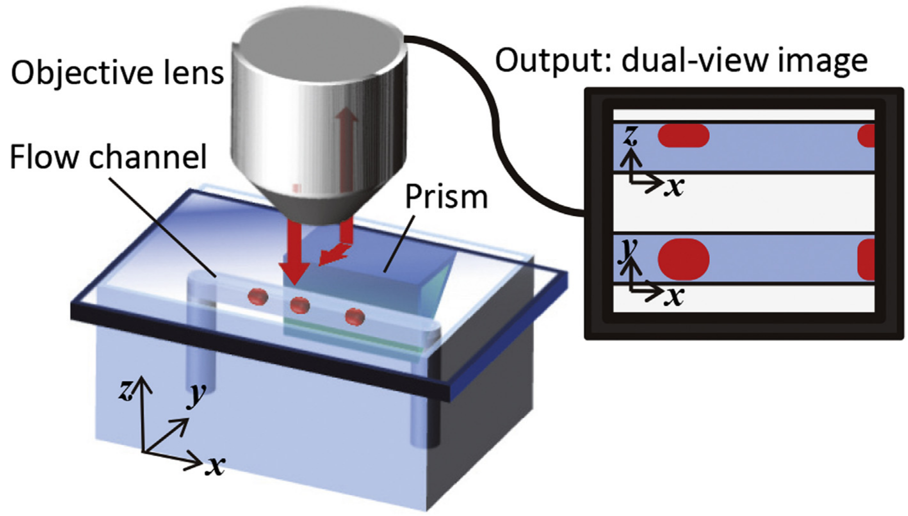

Fig. 1. Concept of dual-view flow-channel visualization. The top (*x*-*y* plane) and side (*x*-*z* plane) views are simultaneously visualized [27]. Reprinted with permission from Transducers Research Foundation. Copyright 2014.

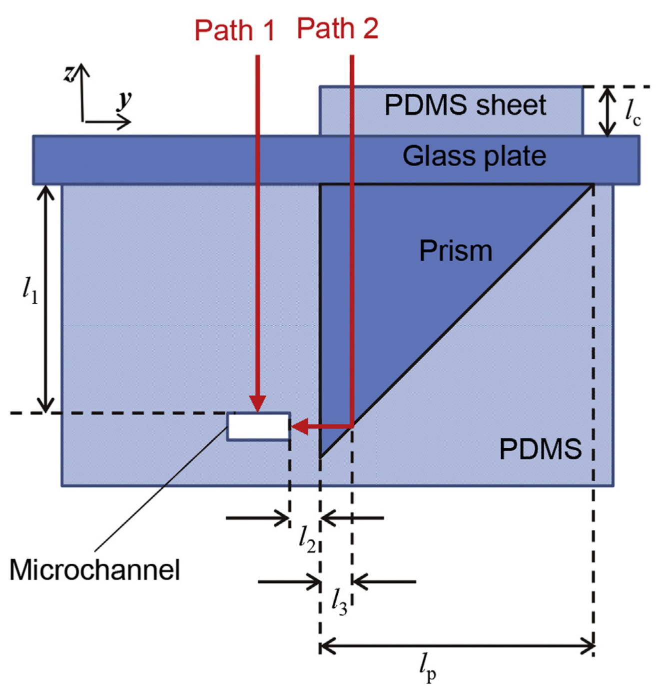

Fig. 2. Side view of the dual-view device. (For interpretation of the references to colour in the text, the reader is referred to the web version of this article.)

pensated by placing a PDMS sheet in the side-view path. First, we considered the focal lengths of the top and side paths and their deviations in different media (PDMS and prism). We then calculated the thickness of the compensating PDMS sheet, and the design was finalized. The device was fabricated, and its validity was confirmed by visualizing the microchannel.

2. Design and model

Fig. 2 shows a side view of the dual-view device. A right-angle prism is used for reflecting the optical path of the side view. In order to fix the prism on a flat surface, the prism is designed to be attached to a glass plate. The tip of the right-angle prism is then used for the reflection of the optical path of the side view to shorten the distance between the microchannel and the reflection point. Since a longer distance would lead to a wider field of view, the microchannel is not placed on the glass plate, but near the tip of the prism.

The two red lines in Fig. 2 denote the optical paths of the top and side views. For the top view (path 1), the microchannel is observed through the glass plate and the PDMS layer between the glass plate and the microchannel (thickness: l_1). For the side view (path 2), the microchannel is observed through the compensating PDMS sheet (thickness: l_c), the glass plate, the prism (side length: l_p), and PDMS layer between the prism and the microchannel (thickness: l_2). The distance between the prism surface (close to the microchannel) and the reflection point of path 2 is defined as l_3. When we ignore the height of microchannel (~several tens of micrometers), the difference between paths 1 and 2 is $l_2 + l_3$.

Despite the difference in path length, the focal lengths of the two paths can be equal by considering refraction at the interfaces. Fig. 3(a) shows a simple model for considering the focal-length shift of refractive elements. In this model, light is introduced from a medium (medium 0) with refractive index n_0 to another medium (medium 1) with refractive index n_1 and a thickness of t at an incident angle of θ. The light then exits medium 1 and re-enters medium 0. The refraction at the interfaces is described by Snell's law,

$$n_0 \sin\theta = n_1 \sin\theta', \tag{1}$$

where θ' is the refractive angle in medium 1.

After passing through medium 1, the locus deviates from the extended line of the incident light, shifting a distance of d such that

$$\frac{d}{t} = 1 - \frac{\tan\theta'}{\tan\theta}. \tag{2}$$

The numerical value of the shift divided by the thickness of medium 1, d/t, is obtained by solving the simultaneous equations. The dependence of the shift/thickness ratio on the incident angle, θ, is represented by the solid line in Fig. 3(b). It was calculated for the case of the air/PDMS interface. Generally, the shift increases for higher incident angles, which suggests that some lens structure is required for at least one of the paths in order to match the two path lengths. In contrast, in the case of a small incident angle where θ (rad) « 1, the approximation $\tan\theta \approx \sin\theta \approx \theta$ can be used and Eq. (2) is written as

$$\frac{d}{t} = 1 - \frac{n_0}{n_1}. \tag{3}$$